



HAL
open science

First passage times in homogeneous nucleation: Dependence on the total number of particles

Romain Yvinec, Samuel Bernard, Erwan Hingant, Laurent Pujo-Menjouet

► To cite this version:

Romain Yvinec, Samuel Bernard, Erwan Hingant, Laurent Pujo-Menjouet. First passage times in homogeneous nucleation: Dependence on the total number of particles. *The Journal of Chemical Physics*, 2016, 144 (3), pp.1-17. <10.1063/1.4940033>. <hal-01353266>

HAL Id: hal-01353266

<https://hal.science/hal-01353266v1>

Submitted on 27 May 2020

HAL is a multi-disciplinary open access archive for the deposit and dissemination of scientific research documents, whether they are published or not. The documents may come from teaching and research institutions in France or abroad, or from public or private research centers.

L'archive ouverte pluridisciplinaire HAL, est destinée au dépôt et à la diffusion de documents scientifiques de niveau recherche, publiés ou non, émanant des établissements d'enseignement et de recherche français ou étrangers, des laboratoires publics ou privés.



HAL Authorization

First passage times in homogeneous nucleation: dependence on the total number of particles

Romain Yvinec¹, Samuel Bernard^{2,3}, Erwan Hingant⁴, Laurent Pujo-Menjouet^{2,3}

¹ PRC INRA UMR85, CNRS UMR7247, Université François Rabelais de Tours, IFCE, F-37380 Nouzilly

² Université de Lyon, CNRS, Université Lyon 1,

Institut Camille Jordan UMR5208, 69622 Villeurbanne, France

³ INRIA Team Dracula, Inria Center Grenoble Rhne-Alpes, France and

⁴ Departamento de Matemática, Universidad Federal de Campina Grande, PB, Brasil.

(Dated: October 19, 2015)

Motivated by nucleation and molecular aggregation in physical, chemical and biological settings, we present an extension to a thorough analysis of the stochastic self-assembly of a fixed number of identical particles in a finite volume. We study the statistic of times it requires for maximal clusters to be completed, starting from a pure-monomeric particle configuration. For finite volume, we extend previous analytical approaches to the case of *arbitrary size-dependent* aggregation and fragmentation kinetic rates. For larger volume, we develop a scaling framework to study the behavior of the first assembly time as a function of the total quantity of particles.

We find that the mean time to first completion of a maximum-sized cluster may have surprisingly a very weak dependency on the total number of particles. We highlight how the higher statistic (variance, distribution) of the first passage time may still help to infer key parameters (such as the size of the maximum cluster) from data. And last but not least, we present a framework to quantify the formation of cluster of macroscopic size, whose formation is (asymptotically) very unlikely and occurs as a large deviation phenomenon from the mean-field limit. We argue that this framework is suitable to describe phase transition phenomena, as *inherent infrequent stochastic processes*, in contrast to classical nucleation theory.

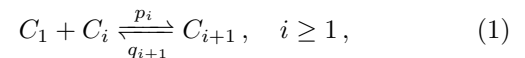
PACS numbers: 02.50.Ga, 82.60.Nh, 87.10.Mn, 87.10.Rt

I. INTRODUCTION

The self-assembly of macromolecules and particles into cluster is a fundamental process in many physical, chemical and biological systems. Although particle nucleation and assembly have been studied for many decades^{1,2}, interest in this field has recently intensified due to engineering, biotechnological and imaging advances at the nanoscale level³⁻⁵. Applications range from material physics to cell physiology and virology (for a detailed list of examples see⁶ and references therein). Many of these applications involve a fixed “maximum” cluster size – of tens to hundreds of units – at which the process is completed or beyond which the dynamics change^{7,8}. One example include the rare self-assembly of mis-folded proteins into fibril aggregate in neurodegenerative diseases (Alzheimer, Parkinson, Prion...)^{9,10}. Developing a stochastic self-assembly model focusing on the formation of a fixed “maximum” cluster size is thus important for our understanding of a large class of biological processes, and the quantification of the variability of the experimental data¹¹⁻¹⁵.

Theoretical models for self-assembly have typically described mean-field concentrations of clusters of all possible sizes using the well-studied mass-action, Becker-Döring equations¹⁶⁻¹⁹. While Master equations for the fully stochastic nucleation and growth problem have been derived, and initial analyses and simulations performed²⁰⁻²⁴, there has been relatively less work on the stochastic self-assembly problem. It has been re-

cently shown that in finite systems, where the maximum cluster size is capped, results from mass-action equations are inaccurate and that in this case a discrete stochastic treatment is necessary^{6,25}. We consider here the Becker-Döring model (BD) defined by the following biochemical reactions



where C_i denotes the number (or concentration) of clusters of size i . Note that in the stochastic version (SBD), the state-space of the system is discrete and finite (see Fig. 1), given by all possible combinations that have a given fixed total number of particles (defined by M , given by the initial condition)

$$\mathcal{E} := \left\{ (C_i)_{i \geq 1} \subset \mathbb{N} : \sum_{i \geq 1} i C_i = M \right\}. \quad (2)$$

The configuration $(C_i(t))_{i \geq 1}$ evolve in continuous time by discrete jumps according to Markovian description of the reactions (1). In our previous examination of first assembly time in this model⁶, we found that a striking finite-size effect arises in the limit of slow self-assembly. In particular, a *faster* detachment rate can lead to a *shorter* assembly time. This unexpected effect arise as the finite-size system may occupy some configurations that have been named “traps”, where no free particle is available and the maximal-size cluster completion may occur only through first a detachment of a particle from a cluster. Discrepancies between the mean-field mass-action approach and the stochastic model were indeed

Comment citer ce document :

Yvinec, R., Bernard, S., Hingant, E., Pujo-Menjouet, L. (2015). First passage times in homogeneous nucleation: dependence on the total number of particles. The Journal of Chemical Physics, 143(18), 184701. PACS numbers: (02.50.Ga) (82.60.Nh) (87.10.Mn) (87.10.Rt).

where $\delta_k^1 = 1$ if $k = 1$ and $\delta_k^1 = 0$ if $k > 1$.

The first assembly time (FAT) for the stochastic discrete Becker-Döring is defined as a first passage time problem²⁹

$$T_{1,0}^{N,M} := \inf\{t \geq 0 : C_N(t) = 1\}. \quad (7)$$

Hence the FAT is the first time to obtain a cluster of size N , starting with a pure single particle initial state, with M particle (see Fig. 1 for an example). To link with macroscopic definition of the nucleation time, we will also consider the generalized first assembly time (GFAT) problems

$$T_{\rho,h}^{N,M} := \inf\{t \geq 0 : C_N(t) \geq \rho M^h\}, \quad (8)$$

for given positive constant ρ and $0 \leq h \leq 1$. Here, we want to analyze the behavior of $T_{\rho,h}^{N,M}$ when $M \rightarrow \infty$, for fixed N , and when both $M, N \rightarrow \infty$. This behavior will depend on scaling on the physical rates p, q , which may naturally depend on the total mass (or volume) of the system³⁰. One way of computing the distribution of first assembly times is to consider the Backward Kolmogorov equation (BKE) describing the evolution of the configuration probabilities as a function of local changes from the initial configuration. The BKE Approach was taken in⁶. It has the advantage to yields exact results for the full distribution of FAT, but it is strictly limited by the size of the system of equations, that grows exponentially with M . In this paper, we rely on exact calculation of simplified reduced models, limit theorems from Eq. (5) for large M and N , and extensive numerical simulations of these equations.

III. RESULTS AND ANALYSIS

Although the state-space (2) of the SBD model (1) is finite, the first passage problem defined by Eq. (8) is in general a very difficult problem: see preliminary studies in^{6,20,21,23}. There are two distinct simplifications that allow the problem to be analytically tractable. We present them here briefly in sections **A** and **B** (and generalize results from⁶). Then we present two asymptotic results for large volume, $M \rightarrow \infty$, with either finite or infinite nucleus size in sections **C** and **D**, respectively. The strategy will be based on re-scaling procedure of the stochastic Eq. (5). Numerical illustrations and results are postponed to the next section.

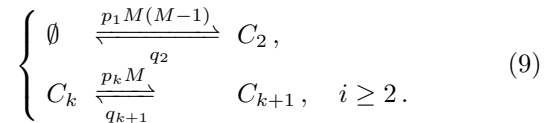
A. Constant Monomer formulation

The SBD model defined by Eq. (5) has the constant mass property

$$\sum_{k \geq 1} k C_k(t) \equiv \sum_{k \geq 1} k C_k(0) = M, \quad t \geq 0.$$

In the original formulation of the BD model (sometimes used in the deterministic context^{17,27}), the total mass

of the system is not preserved, but rather the quantity of free particles (think *e.g.* of a source/sink that will keep instantaneously constant the quantity of available free particles). We will refer to this formulation as the constant monomer stochastic Becker-Döring model (CMSBD). We can represent it by the following reactions



In the above formulation, $C_1(t) \equiv M$ is now a constant over time. Note that we expect such model to be close to the original SBD (for small times, up to the FAT) in the limit of large number of particle M . The main advantage of the constant monomer formulation is to be linear and hence analytically solvable. Indeed, it is known that for linear population model³¹, the number of individuals in each subclass of the population (starting with no individuals at time 0), namely here $C_2(t), \dots, C_N(t), \dots$, are independent Poisson random variable. Moreover, for this model (9), the mean $c_2(t), \dots, c_N(t), \dots$ are solution of the linear equation, given for all $t \geq 0$, by

$$\frac{d}{dt} c_k(t) = j_{k-1}(t) - j_k(t), \quad \forall k \geq 2, \quad (10)$$

with

$$\begin{cases} j_1(t) = p_1 M(M-1) - q_2 c_2(t), \\ j_k(t) = p_k M c_k(t) - q_{k+1} c_{k+1}(t) \quad \forall k \geq 2, \end{cases} \quad (11)$$

and initial condition $c_k(0) = 0$ for all $k \geq 2$. Note that the last set of Eq. (10)-(11) is very close to the deterministic Becker-Döring model (3)-(4) taking $c_1 \equiv M$. To calculate the FAT $T_{1,0}^{N,M}$ we use the survival function

$$\begin{aligned} S_{1,0}^{N,M}(t) &:= \mathbb{P}\{T_{1,0}^{N,M} > t\} \\ &= \mathbb{P}\{C_N(s) = 0, s \leq t \mid C_k(0) = M\delta_{k=1}\}. \end{aligned}$$

Then, using an absorbing boundary condition at $k = N$ ($q_N = p_N = 0$) together with the initial condition entail that $C_N(t) = 0$ for some $t \geq 0$ if and only if $C_N(s) = 0$ for all $s \leq t$, so that

$$S_{1,0}^{N,M}(t) = \mathbb{P}\{C_N(t) = 0 \mid C_k(0) = M\delta_{k=1}\}.$$

Finally, since $C_N(t)$ is Poisson distributed (linear system) with mean $c_N(t)$, we have

$$S_{1,0}^{N,M}(t) = e^{-c_N(t)}. \quad (12)$$

Equations (10)-(11) with the absorbing boundary at $k = N$ can be rewritten as a linear system

$$\begin{cases} \dot{\mathbf{c}} = \mathbf{A}\mathbf{c} + \mathbf{B}, \\ \dot{c}_N(t) = p_{N-1} M c_{N-1}(t), \end{cases} \quad (13)$$

where $\mathbf{c} = (c_2, c_3, \dots, c_{n-1})^T$, $\mathbf{B} = (p_1 M(M-1), 0, \dots, 0)^T$ and \mathbf{A} is a tridiagonal matrix with elements

$$\begin{cases} a_{k,k} = -q_{k+1} - p_{k+1}M, \\ a_{k+1,k} = p_{k+1}M, \\ a_{k,k+1} = q_{k+1}. \end{cases}$$

The study of the linear system (13) has been performed both for the infinite dimensional case³² and for the truncated case³³. In particular, it is shown that a similarity transformation

$$\mathbf{A} = \mathbf{DSD}^{-1}$$

with $D = \text{diag}(\sqrt{\tilde{Q}_k M^k})$ and $\tilde{Q}_k = \prod_{j=2}^k \frac{p_{j-1}}{q_j}$ leads to a matrix \mathbf{S} real symmetric tri-diagonal with non-zero elements on the sub and super-diagonal. Hence, classical linear algebra results shows that the eigenvalues of \mathbf{A} are real and distinct. Then, a general form of $c_N(t)$ is given by

$$c_N(t) = p_{N-1}M \left[\sum_{k=1}^{N-2} \alpha_k V_{N-2}^{(k)} \frac{e^{\lambda_k t} - 1}{\lambda_k} - (\mathbf{A}^{-1}\mathbf{B})_{N-2} t \right].$$

where λ_k, V^k denotes the eigenelements of \mathbf{A} and α_k are determined by initial conditions. Analytical solutions are available¹² for constant coefficient only (the matrix \mathbf{A} is in such case a Toeplitz matrix, with constant diagonal values, see Annex A.1). However, asymptotic expression are valid in the general cases. In particular, we have for small times $c_2(t) = p_1 M(M-1)t + o(t)$ and

$$\dot{c}_k = p_{k-1}M c_{k-1} + o(t),$$

so that, for $t \ll 1$,

$$c_N(t) \approx_{t \ll 1} M^N \prod_{k=1}^{N-1} p_k \frac{t^{N-1}}{(N-1)!},$$

and Eq. (12) is thus the survival function of a Weibull distribution, of shape parameter $k = N-1$ and scale parameter $\lambda = ((N-1)! / (M^N \prod_{k=1}^{N-1} p_k))^{1/(N-1)}$. Hence, we get

$$\langle T_{1,0}^{N,M} \rangle \approx_{M \rightarrow \infty} \frac{\Gamma(1 + 1/(N-1))}{\left(\prod_{k=1}^{N-1} p_k\right)^{1/(N-1)}} \frac{((N-1)!)^{1/(N-1)}}{M^{1+1/(N-1)}}. \quad (14)$$

Variance formula for the Weibull distribution yields the asymptotic coefficient of variation (standard deviation over the mean)

$$cv_{T_{1,0}^{N,M}} \approx_{M \rightarrow \infty} \sqrt{2(N-1) \frac{\Gamma(2/(N-1))}{\Gamma(1/(N-1))^2} - 1}. \quad (15)$$

Note in particular that the coefficient of variation do not vanish in large population, and that it is independent of

the particular shape of the aggregation rate and depends only on the size of the maximal cluster N .

For the generalized first assembly time GFAT, similar time scale asymptotic on the Eq. (13) on the mean gives the following expression

$$\langle T_{\rho,h}^{N,M} \rangle \approx_{M \rightarrow \infty} \frac{C(p,N)}{M} \frac{1}{M^{(1-h)/(N-1)}}, \quad (16)$$

where $C(p,N)$ is a constant that depends only on N and the aggregation rates $p_k, k \leq N$ (that can be made explicit if the full solution of Eq. (13) is known). Those asymptotic expressions are illustrated in Annex (Fig. A.1) where a perfect match is observed with numerical simulations.

B. Single cluster model

Another simplified model that can be analytically solved for the FAT problem is given by the assumption that a single cluster can be formed at a time^{6,34}. We expect such model to be close to the original model when the fragmentation dominates, so that formation of many (large) cluster is unlikely. In such model, called the single-cluster stochastic Becker-Döring (SCSBD) model we may represent only the size of the single cluster, so that the state space is now one dimensional, being simply

$$\mathcal{E}_1 := [1, \dots, N],$$

and the possible reactions are given by (k denotes the size of the single cluster)

$$\begin{cases} k = 1 \xrightarrow{\frac{p_1 M(M-1)}{q_2}} k = 2, \\ k \xrightarrow{\frac{p_k(M-k)}{q_{k+1}}} k+1, \quad k \geq 2. \end{cases} \quad (17)$$

In such a scenario, exact solution and classical First Passage Theory³⁰ gives (it is a one-dimensional discrete random walk)

$$\langle T_{1,0}^{N,M} \rangle = \sum_{i=1}^{N-1} \sum_{j=1}^i \frac{\prod_{k=j+1}^i q_k}{\prod_{k=j}^i p_k} \frac{1}{M^{\delta_j} \prod_{k=j}^i (M-k)}. \quad (18)$$

In addition, general formula for variance and cumulative distribution function are available³⁵. Those theoretical expressions are illustrated in Annex (Fig. A.2) where a perfect match is observed with numerical simulations.

Asymptotic expressions of the mean assembly time is straightforwardly deduced from Eq. (18). For instance, assume $q_k = \frac{\bar{q}_k}{\varepsilon}$ and that $\varepsilon \rightarrow 0$, the leading order of the mean assembly time is

$$\langle T_{1,0}^{N,M} \rangle \approx_{\varepsilon \rightarrow 0} \frac{1}{\varepsilon^{N-2}} \frac{\prod_{k=2}^{N-1} \bar{q}_k}{\prod_{k=1}^{N-1} p_k \prod_{k=0}^{N-1} (M-k)}.$$

Also, one can show that in the asymptotic $\varepsilon \rightarrow 0$, for large fragmentation rate, the FAT $T_{1,0}^{N,M}$ is an exponential distribution⁶.

Finally, for large N and M , we can rescale the sum in Eq. (18) to obtain a suitable expression for the mean FAT when $N \rightarrow \infty$. Assume that the aggregation rates scale with M so that $p_1 = \bar{p}_1/M^2$, $p_k = \bar{p}_k/M$, $k \geq 2$. Then, let us introduce the rescaled size variable $x = k/N$, and define the rescaled kinetic rate

$$\begin{aligned}\bar{p}(x) &= \sum_{k \geq 2} \bar{p}_k \mathbf{1}_{[k/N, (k+1)/N)}(x), \\ q(x) &= \sum_{k \geq 2} q_k \mathbf{1}_{[k/N, (k+1)/N)}(x),\end{aligned}$$

we have, for $N = \sqrt{M} \rightarrow \infty$ (see details in Annex, section A.2.2),

$$\begin{aligned}\langle T_{1,0}^{\sqrt{M}, M} \rangle &\approx_{M \rightarrow \infty} M \int_0^1 \int_0^y \frac{e^{(y^2-z^2)/2}}{q(y)} \\ &\exp \left[\sqrt{M} \int_z^y \ln \left(\frac{q(x)}{\bar{p}(x)} \right) dx \right] dy dz. \quad (19)\end{aligned}$$

In particular, when $q(x) > \bar{p}(x)$ on an interval of positive measure on $[0, 1]$, the last expression (19) implies that the mean FAT to reach the *macroscopic* size $x = 1$ ($k = N = \sqrt{M}$) is exponentially large as $M \rightarrow \infty$. As an example, suppose that $q > \bar{p}$ are size-independent. Then, Eq. (19) becomes

$$\langle T_{1,0}^{\sqrt{M}, M} \rangle \approx_{M \rightarrow \infty} \frac{M}{q} \int_0^1 \int_0^y e^{(y^2-z^2)/2} \left(\frac{q}{\bar{p}} \right)^{\sqrt{M}(y-z)} dy dz.$$

Those theoretical expressions are illustrated in Annex (Fig. A.3 and A.4). Note that a different approach is to link the one-dimensional discrete random walk (17) with a one-dimensional stochastic differential equation, and to use Large Deviation Theory to derive asymptotic FAT³⁴ (Annex, section A.2.3). This scaling approach and the link with a continuous size model when $N \rightarrow \infty$ will be taken on the full SBD model in section D.

C. Large M , finite N

In this section, we investigate the behavior of the SBD and its FAT when the total number of particles M tends to infinity, while the size N of the maximal cluster to reach stay finite. We distinguish two scenario, which yields distinct results. In the first one, the aggregation and fragmentation rate p_k, q_k are taken independent of M . As the aggregation propensities increase with M , it is expected that the FAT decrease to 0 as $M \rightarrow \infty$. The objective is to find valid asymptotic expression, and its dependence with respect to other parameters, like the maximal cluster size N for instance. In the second case, the aggregation rate is scaled with the total number of particles, with $p_k = \frac{\bar{p}_k}{M}$. This scaling is motivated by classical

system size expansion of chemical reaction networks³⁰. As the total number of particles increases, the volume also increases so that the overall reaction propensities of the aggregation reactions stay constant. In such case, one expect to recover the deterministic first passage time of the classical deterministic BD model.

Let us now introduce our general rescaling strategy. The number of cluster of size k , given by C_k , are rescaled into

$$D_k^M(t) = \frac{C_k(t/M^\gamma)}{M}$$

with γ a scaling coefficient to be chosen latter. Then, from Eq. (5)-(6), we obtain, for any $t \geq 0$,

$$\begin{cases} D_1^M(t) = 1 - 2J_1^M(t) - \sum_{k \geq 2} J_k^M(t), \\ D_k^M(t) = J_{k-1}^M(t) - J_k^M(t), \quad k \geq 2, \end{cases} \quad (20)$$

with

$$\begin{aligned}J_k^M(t) &= \frac{1}{M} Y_k^+ \left(\int_0^t M^{2-\gamma} p_k D_1^M(s) (D_k^M(s) - M^{-1} \delta_k^1) ds \right) \\ &- \frac{1}{M} Y_{k+1}^- \left(\int_0^t M^{1-\gamma} q_{k+1} D_{k+1}^M(s) ds \right), \quad k \geq 2. \quad (21)\end{aligned}$$

We recall a standard result of convergence of Poisson Processes (law of large numbers³⁶), that

$$\frac{1}{n} Y(nt) \xrightarrow{n \rightarrow \infty} t,$$

where Y is a standard Poisson Process.

1. No scaling of the aggregation rate

Using $\gamma = 1$, and the standard law of large numbers applied to the Eq. (20)-(21), we can show³⁷ (see Annex, section 3) that the sequence of stochastic processes $(D_k^M(t))$ converges, as $M \rightarrow \infty$, in a rigorous sense (in the trajectory space) to the solution of the irreversible aggregation deterministic model (BD with $q_k = 0$), given, for all $t \geq 0$, by

$$\begin{cases} \frac{d}{dt} d_1 = -2j_1(t) - \sum_{k \geq 2} j_k(t), \\ \frac{d}{dt} d_k = j_{k-1}(t) - j_k(t), \quad \forall k \geq 2, \end{cases} \quad (22)$$

with

$$j_k(t) = p_k d_1 d_k(t), \quad \forall k \geq 1, \quad (23)$$

and initial condition $d_1(0) = 1$ and $d_k(0) = 0$, for all $k \geq 2$. Intuitively, in the rescaled variable D_k^M , the aggregation process is much more favorable compared to the fragmentation because the number of free particles is very large. By definition of the GFAT Eq. (8), with $h = 1$,

$$MT_{\rho,1}^{N,M} = \inf\{t \geq 0 : D_N^M(t) \geq \rho\}.$$

Then, using the convergence of $(D_k^M(t))$, we obtain the following asymptotic behavior of the GFAT for $h = 1$,

$$\lim_{M \rightarrow \infty} MT_{\rho,1}^{N,M} = \inf\{t \geq 0 : d_N(t) \geq \rho\}. \quad (24)$$

The latter quantity is deterministic, and may be finite or infinite, according to the respective value of p_k, N and ρ .

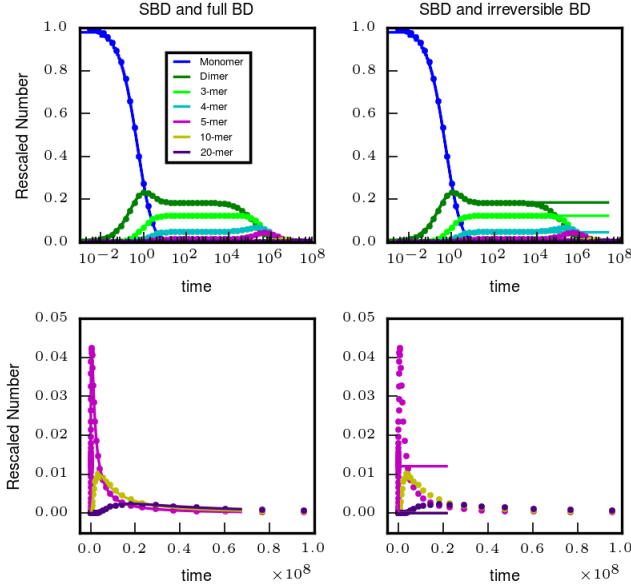


FIG. 2: SBD and BD Trajectories. For the SBD, we simulate the rescaled Eq. (20)-(21), with $M = 10^{5.5}$, and kinetic rates are $p_k \equiv 1$ for all $k \geq 1$ and $q_k \equiv 1$ for all $k \geq 2$. For the BD model, we simulate on the left columns the full BD Eq. (22)-(26) and on the right columns the irreversible BD Eq. (22)-(23). The rescaled SBD trajectories are plotted with filled circles, together with the corresponding BD trajectories in plain lines, for the monomer and i -cluster, $i = 2, 3, 4, 5, 10, 20$, according to the legend. The lower panel correspond to the same numerical simulation of the upper panel, with a zoom on the y -axis to improve the visualization of the i -cluster for $i = 5, 10, 20$. It is immediate to see that the full BD Eq. (22)-(26) agrees perfectly with the rescaled SBD Eq. (20)-(21) for all time, while the irreversible BD Eq. (22)-(23) matches only up to a time scale of order M .

The limit model (22)-(23) do not capture the FAT and the GFAT $T_{\rho,h}^{N,M}$ for $h < 1$ (such event is reached for time $t = 0^+$). However, as the initial number of monomers is large, we can use an intermediate approximation of the dynamic of the stochastic model, as a hybrid deterministic/stochastic model. First, note that pure coagulation BD model (22)-(23) have been extensively studied³⁸, where exact time-dependent solution for $p_k = pk$ are given, and time asymptotic behavior are given for power law coefficient $p_k = pk^\lambda$, $0 \leq \lambda \leq 1$. We restrict the following discussion to the constant rate case, $\lambda = 0$, for simplicity (results are analogous in the power law case). In such case, the stationary state of the pure coagulation

BD model^{17,38} (22)-(23) is $d_1^* = 0$ and

$$d_k^* = \frac{k-1}{ek!}, \quad k \geq 2. \quad (25)$$

Although the rescaled threshold ρM^{h-1} will be reached by d_N (and hence by D_N^M) for any ρ and $h < 1$ for large enough M (as $d_N^* > 0$), one can already see that for “intermediate” M , we may have $Md_N^* \ll 1$, so that the threshold may not have been reached while the free particle have vanished ($d_1^* = 0$). In such case, it is necessary to take into account the small but crucial contribution of the aggregate shortening. For that, let us consider as a further approximation of Eq. (20)-(21) the following deterministic model (still with constant rate coefficients, to simplify the following), given, for all $t \geq 0$, by Eq. (22) and flux definition

$$j_k(t) = pd_1(t)d_k(t) - \frac{1}{M}qd_{k+1}(t), \quad k \geq 1, \quad (26)$$

where $1/M$ is seen as a small parameter. To obtain results for the quantity $T_{\rho,h}^{N,M}$ for any $h < 1$, we need to study the time-dependent properties of the favorable aggregation limit $M \rightarrow \infty$ of the deterministic BD model Eq. (22)-(26). The following discussion is illustrated with Fig. 2 (see also in Annex, Fig. A.7, A.8). For constant rate p, q , it is known¹⁷ that under favorable aggregation limit $q/M \ll p$, the deterministic BD model Eq. (22)-(26) exhibits the following successive periods:

- Firstly, the model behaves as the irreversible aggregation BD model, Eq. (22)-(23), during a time-scale of order $e \log(M)$, until monomer concentration $d_1(t)$ becomes small;
- Secondly, when the monomer concentration d_1 is of order $1/M$, there is a metastable period in which each concentration species of size $k \geq 2$ are nearly constant, equal to d_k^* , the equilibrium state Eq. (25) of the irreversible aggregation BD model, Eq. (22)-(23). The concentration $d_k(t)$ stays roughly constant to the values d_k^* , distinct from the steady-state values of the full BD Eq. (22)-(26), until the next time scale;
- Thirdly, at a time scale of order M (which is the time scale of aggregate shortening), larger aggregates are created within a process akin to diffusion in the size k -space (slow redistribution of aggregate sizes);
- Finally, every concentration species d_k reaches the classical steady-state value of the full BD Eq. (22)-(26) within a time scale of order M^2 . Steady-state values \bar{d}_k are given by

$$\bar{d}_k = \left(\frac{pM}{q}\right)^{k-1} \bar{d}_1^k, \quad k \geq 2,$$

where \bar{d}_1 is determined by the mass conservation property. Such values can be approximated by $\bar{d}_1 \approx 1/M$ and $\bar{d}_k \approx 1/M(1 - 1/\sqrt{M})^{k-1}$.

To approximate the GFAT $T_{\rho,h}^{N,M}$, we need to know in which of these periods the event $\{C_N(t) \geq \rho M^h\}$ is

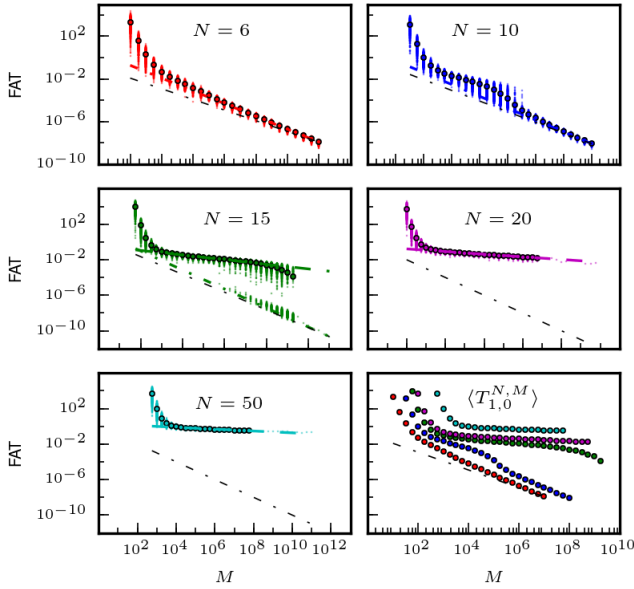


FIG. 3: First Assembly Time $T_{1,0}^{N,M}$ for the original SBD (section III C 1) as a function of the total mass M (in log-log scale) for five different maximal cluster sizes $N \in \{6, 10, 15, 20, 50\}$. Each color light dot is a single realization of the FAT. For each condition, large circles represent the statistical mean over 1000 samples (A few condition are sampled only once, namely for $N = 15, 20, 50$ and large M , for which the mean is not shown). Black dash-dotted lines are straight lines of slope -1 , color dash-dotted lines are straight lines of slope $-(1 + 1/(N - 1))$ (as in Eq. (14)). And for $N = 15, 20, 50$ we plot additionally dashed lines of slope resp. $-0.26, -0.15$ and -0.10 . The last panel in bottom-right represent the 5 mean FAT on the same scale. Kinetic rates are $p_1 = 0.5$, $p_k \equiv 1$, and $q_k \equiv 100$ for all $k \geq 2$.

A. The First Assembly Time can be weakly-dependent on the total number of monomer M , and highly variable even in large population

We begin with the analysis of the FAT as a function of the total number of monomer M , when the maximal cluster size N and the aggregation rates p_k are fixed. For $N = 6, 10, 15$, the prediction of the asymptotic behavior of $T_{1,0}^{N,M}$, the waiting time for a single maximal cluster to be formed, is verified: the mean FAT decrease linearly in log-log scale as M increase, with a slope equal to $-(1 + 1/(N - 1))$, as in the linear CMSBD model (Fig. 3, upper panels), see Eq. (14). The coefficient of variation (cv, standard deviation over the mean), that measures the variability of the FAT, is also consistent with a transition from an exponential distribution to a Weibull distribution as M increases: the cv decreases from 1 to the predicted value by Eq. (15) (Fig. 4, and Fig. A.1 in Annex for the CMSBD). Furthermore, one can observe very clearly for $N = 15$ the bimodal behavior predicted for large but intermediate M values (Fig. 3, third panel). For M from 10^6 to 10^{10} , the sampled FAT

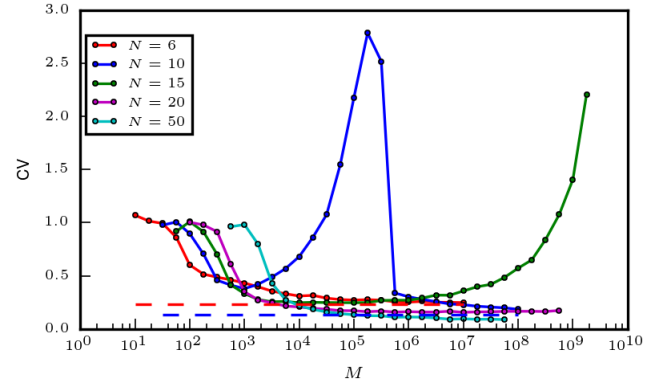


FIG. 4: Coefficient of Variation (CV) for the First Assembly Time $T_{1,0}^{N,M}$ as a function of the total mass M corresponding to the realizations of Fig 3. For $N = 6, 10$ we plot additionally horizontal dashed lines at the value predicted by the Weibull distribution, see Eq. (15).

segregates between two groups separated by several order of magnitude (one group below 10^{-6} , one group around $10^{-2}, 10^{-3}$). The higher values of the sampled FAT corresponds to trajectories that went through the threshold $C_N = 1$ after the metastable period described in paragraph III C 1. For $N = 20$ and $N = 50$, we could simulate in a reasonable computation time (several weeks) only up to $M = 10^{13}$ and $M = 10^{11}$ respectively. Below these values, the metastable states computed in table II predict that the threshold will be mostly reached after the metastable period, which explain the large 'plateau' observed for the FAT up to M^{13} (resp M^{11}): the FAT is nearly independent of M on a broad range of values (Fig. 3, the slope for $N = 15, 20, 50$ are resp. approximately $-0.26, -0.15, -0.10$). The bimodal behavior observed for the FAT for $N = 10, 15$ can also be visualized on the cv, which results in a large peak of the cv values for intermediate M values (Fig. 4). Trajectories of the number of cluster as a function of time help to visualize the different phases. We illustrate in Annex, Fig. A.7, A.8, stochastic trajectories of the SBD model together with the favorable aggregation limit of the deterministic BD model, in order to clearly identify the metastable period. In Fig. A.9 and A.10, we exhibit two trajectories of the stochastic SBD model that results in two FAT that differ from several log of order of magnitude, due to the metastable period. We also point the accuracy of the approximation by a linear model that has for initial condition the metastable state. Finally, the transition from an exponential distribution to a Weibull distribution as M increases, trough an intermediate bimodal distribution, is also illustrated on Histogramms of the FAT over 10^3 realization in Fig. A.11.

Similar results are obtained for the GFAT $T_{\rho,h}^{N,M}$, where the linear log-dependence with a slope $-(1 + (1-h)/(N-1))$ (see Eq. (16) for the CMSBD model) is found to be perfectly satisfied for $N = 3, 5$ and $h = 0.25, 0.5, 0.75$ and

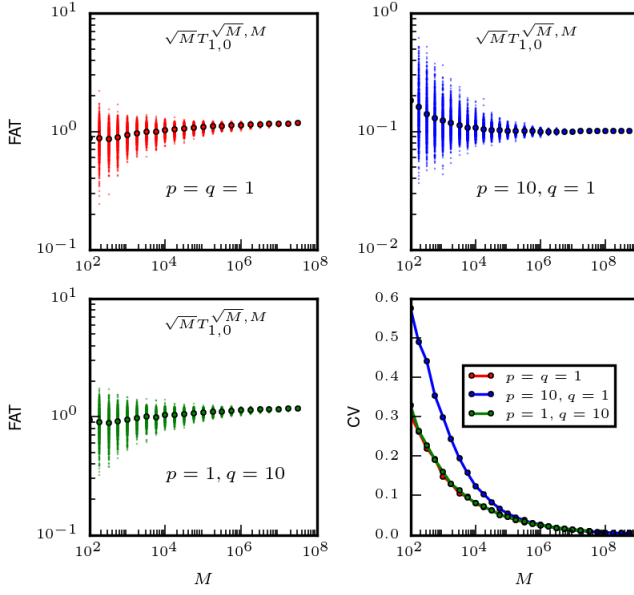


FIG. 7: First Assembly Time $T_{1,0}^{\sqrt{M},M}$ for the original SBD and large maximal cluster size of order $N = \sqrt{M}$ (section III D 1) as a function of the total mass M (in log-log scale) for three different kinetic rates $(p_k, q_k) \in \{(1, 1); (10, 1); (1, 10)\}$. The FAT is multiplied by \sqrt{M} to verify the scaling in Eq. (32). Finally, the panel in bottom right represent the Coefficient of Variation (CV) as a function of the total mass M corresponding to the realizations of the first three panels (top and bottom left).

ation may occur if the aggregation is not favorable compared to the fragmentation, as in the SCSBD model (17) (Annex, Fig. A.4). Indeed, in such case, the deterministic limit (33) predicts that the FAT is never reached (and equals ∞) as the drift is negative for small (macroscopic) size x . For the finite system, the FAT grows exponentially fast with M , in agreement with Eq. (19). On the right panels in Fig. 9, we show few time-dependent trajectories that are representative of a phase-transition phenomena, with a very abrupt change of phase, occurring at a widely variable time (the cv is near 1). Although the deterministic limit predicts that the aggregation will *not* take place (and the monomer number will not decrease), in the SBD model the aggregation is *always* complete (no monomer at the end), but at larger and larger time as M is increasing.

V. SUMMARY AND CONCLUSIONS

We have studied the problem of determining the First Assembly Time (FAT) of a cluster of a pre-determined size N to form from an initial pool of M independent monomers characterized by size-dependent attachment and detachment rates p_k and q_k , respectively. We have developed a full stochastic approach, based on the

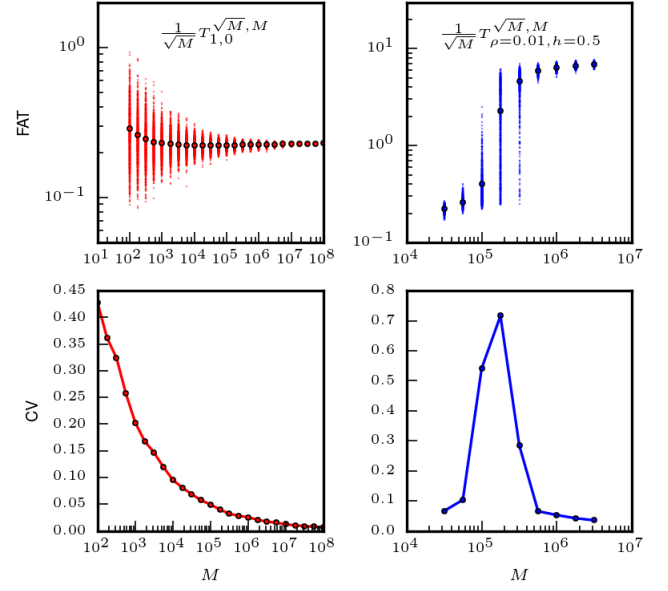


FIG. 8: First Assembly Time $T_{1,0}^{\sqrt{M},M}$ (top left) and Generalized First Assembly Time $T_{\rho,h}^{\sqrt{M},M}$ (top right) for the rescaled SBD and large maximal cluster size of order $N = \sqrt{M}$ (section III D 2) as a function of the total mass M (in log-log scale). Kinetics rates are $p(x) \equiv 5$ and $q(x) = x$. Both the FAT and the GFAT are divided by \sqrt{M} to verify the scaling in Eq. (34). Finally, the panels in bottom left and right represent the Coefficient of Variation (CV) as a function of the total mass M corresponding to the realizations of the upper panels.

stochastic Becker Döring equations (SBD).

We developed two simplified model and were able to find exact results for the FAT statistics for general values of M, N and p_k, q_k . The first simplification is to consider that the number of monomer stays constant over time (linear CMSBD model). The FAT was found to be asymptotically (for large M) a Weibull distribution, and the mean GFAT decrease to 0 as M increase to infinity with a log-linear dependence, with coefficient $1 + (1 - h)/(N - 1)$, for any $h \in [0, 1]$, and any N . The second simplification is to consider that a single cluster can be formed at a time (SCSBD). The FAT was found to be asymptotically an exponential distribution (for large detachment rate q_k), and the mean FAT increase to ∞ as q increase to infinity with a log-linear dependence, with coefficient $N - 2$, for any N . We also show that in the case of unfavorable aggregation ($q_k > p_k$), the formation of large cluster takes an exponentially large time as M increases to ∞ .

With the analytical results on the simplified model in mind, we analyzed the behavior of the FAT for the full SBD. Using a rescaling strategy, as the total number of monomer M increases to ∞ , we found asymptotic expression of the mean FAT and GFAT as a function of a first passage time associated to deterministic models,

- ¹ R. Becker and W. Döring, Kinetische behandlung der keimbildung in übersättigten dämpfen, *Annalen der Physik* **24** 719-752 (1935).
- ² J. Kuipers, Theory and Simulation of Nucleation, *Utrecht University Repository Ph.D.* (2009).
- ³ G. M. Whitesides and M. Boncheva, Beyond molecules: self-assembly of mesoscopic and macroscopic components, *Proc. Natl. Acad. Sci. USA* **99** 4769-4774 (2002).
- ⁴ G. M. Whitesides and B. Grzybowski, Self-assembly at all scales, *Science* **295** 2418-2421 (2002).
- ⁵ R. Groß and M. Dorigo, Self-assembly at the macroscopic scale, *Proc. IEEE* **96** 1490-1508 (2008).
- ⁶ R. Yvinec, M. R. D'Orsogna and T. Chou, First passage times in homogeneous nucleation and self-assembly, *J. Chem. Phys.*, **137** 24 (2012)
- ⁷ M. Gibbons, T. Chou, M. R. D'Orsogna, Diffusion-dependent mechanisms of receptor engagement and viral entry, *J. Phys. Chem. B* **114** 15403-15412 (2010).
- ⁸ N. Hoze and D. Holman, Kinetics of aggregation with a finite number of particles and application to viral capsid assembly, *J. Math. Biol.* **70** 7 1685-1705 (2015).
- ⁹ C. Soto, Unfolding the role of protein misfolding in neurodegenerative diseases, *Nature Rev. Neurosci.* **4** 49-60 (2003).
- ¹⁰ J. Masela, V.A.A. Jansena and M. A. Nowak, Quantifying the kinetic parameters of prion replication, *Biophys. Chem* **77** 139-152 (1999).
- ¹¹ E. T. Powers and D. L. Powers, The kinetics of nucleated polymerizations at high concentrations: amyloid fibril formation near and above the supercritical concentration, *Biophys. J.* **91** 122-132 (2006).
- ¹² R. Yvinec, Probabilistic modelisation in molecular and cellular biology, *Université Lyon 1 Ph.D.* tel-00749633 (2012)
- ¹³ E. Hingant, Contributions la modlisation mathmatique et numrique de problmes issus de la biologie - Applications aux Prions et la maladie d'Alzheimer, *Université Lyon 1 Ph.D.* tel-00763444 (2012)
- ¹⁴ W.-F. Xue, S. W. Homans and S. E. Radford, Systematic analysis of nucleation-dependent polymerization reveals new insights into the mechanism of amyloid self-assembly, *Proc. Natl. Acad. Sci. USA*, **105** 26 8926-31 (2008)
- ¹⁵ T. P. J. Knowles et al. An analytical solution to the Kinetics of Breakable filament assembly, *Science*, **1533** 2009 1533-7 (2010)
- ¹⁶ O. Penrose, The Becker-Döring equations at large times and their connection with the LSW theory of coarsening, *J. Stat. Phys.* **89** 305-320 (1997).
- ¹⁷ J. A. D. Wattis and J. R. King, Asymptotic solutions of the Becker-Döring equations, *J. Phys. A: Math. Gen.* **31** 7169-7189 (1998).
- ¹⁸ P. Smereka, Long time behavior of a modified Becker-Döring system, *J. Stat. Phys.* **132** 519-533 (2008).
- ¹⁹ T. Chou and M. R. D'Orsogna, Coarsening and accelerated equilibration in mass-conserving heterogeneous nucleation, *Phys. Rev. E* **84** 011608 (2011).
- ²⁰ F. Schweitzer, L. Schimansky-Geier, W. Ebeling, and H. Ulbricht, A stochastic approach to nucleation in finite systems: theory and computer simulations, *Physica A* **150** 261-279 (1988).
- ²¹ F.P. Kelly, Reversibility and stochastic networks, *Cambridge Mathematical Library* (1979)
- ²² A. H. Marcus, Stochastic Coalescence, *Technometrics*, **10** 133-143 (1968).
- ²³ J. S. Bhatt and I. J. Ford, Kinetics of heterogeneous nucleation for low mean cluster populations, *J. Chem. Phys.* **118** 3166-3176 (2003).
- ²⁴ A. A. Lushnikov, Coagulation in Finite Systems, *J. Coll Inter. Scie.* **65** 276-285 (1978).
- ²⁵ M. R. D'Orsogna, G. Lakatos, and T. Chou, Stochastic self-assembly of incommensurate clusters, *J. Chem. Phys.* **136** 084110 (2012).
- ²⁶ V. Calvez, N. Lenuzza, M. Doumic, J-P Deslys, F. Mouthon and B. Perthame, Prion dynamics with size dependency-strain phenomena, *J. biol. dyn.*, **4** 1751-3766 (2010)
- ²⁷ J.M. Ball, J. Carr and O. Penrose, The Becker-Döring Cluster Equations: Basic Properties and Asymptotic Behaviour of Solutions, *Commun. Math. Phys.* , **104** 4 (1986)
- ²⁸ P. Laurençot and S. Mischler, From the Becker-Döring to the Lifshitz-Slyozov-Wagner Equations, *J. Stat. Phys.*, **106** 5-6 (2002)
- ²⁹ S. Redner, A guide to first passage processes, *Cambridge University Press*, (2001).
- ³⁰ N. Van Kampen, Stochastic Processes in Physics and Chemistry, 3rd Edition, *North Holland* (2007)
- ³¹ J. F. C. Kingman, Markov Population Processes, *J. Appl. Prob.* **6** 1-18 (1969).
- ³² M. Kreer, Classical BeckerDöring cluster equations: Rigorous results on metastability and longtime behaviour, *Annalen der Physik* , **2** 398-417 (1993)
- ³³ D. B. Duncan and R. M. Dunwell, Metastability in the Classical, Truncated Becker-Döring Equations, *Proceedings of the Edinburgh Mathematical Society* , **45** 701-716 (dat2002e)
- ³⁴ O. Penrose, Nucleation and droplet growth as a stochastic process, in Analysis and Stochastics of Growth Processes and Interface Models, *Oxford University Press*, (2008)
- ³⁵ D. T. Gillespie, Transition time statistics in simple bistable chemical systems, *Physica A: Statistical Mechanics and its Applications* , **101** 2 (1980)
- ³⁶ D. F. Anderson and T. G. Kurtz, Models of biochemical reaction systems in Stochastic Analysis of Biochemical Systems, *Springer International Publishing* (2015)
- ³⁷ I. Jeon, Existence of Gelling Solutions for Coagulation-Fragmentation Equations, *Commun. Math. Phys.* , **567** 541-567 (1998)
- ³⁸ N. V. Brilliantov and P. L. Krapivsky, Nonscaling and source-induced scaling behaviour in aggregation model of movable monomers and immovable clusters, *J. Phys. A* , **4789** (1991)
- ³⁹ J. Deschamps, E. Hingant and R. Yvinec, Boundary value for a nonlinear transport equation emerging from a stochastic coagulation-fragmentation type model, *arXiv:1412.5025*, (2015)
- ⁴⁰ A. Vasseur, F. Poupaud, J-F Collet and T. Goudon, The Beker-Döring System and its Lifshitz-Slyozov Limit, *SIAM J. Appl. Math.*, **62** 5 (2002)
- ⁴¹ J-F Collet, Some modelling issues in the theory of fragmentation-coagulation systems, *Commun. Math. Sciences*, **1** 35-54 (2004)
- ⁴² A. B. Bortz, M. H. Kalos, and J. L. Lebowitz, A new algorithm for Monte Carlo simulation of Ising spin systems,

Comment citer ce document :

Yvinec, R., Bernard, S., Hingant, E., Pujol-Menjouet, L. (2015). First passage times in homogeneous nucleation: dependence on the total number of particles. The Journal of Chemical Physics, PACS number(s) 02.50.Ga B2160106387.49400337.10.Rt).

- J. Comp. Phys.* **17** 10-18 (1975).
- ⁴³ D.T. Gillespie, Exact Stochastic Simulation of Coupled Chemical Reactions, *J. Phys. Chem.* **81** 2340-2361 (1977).
- ⁴⁴ M. A. Gibson and J. Bruck, Efficient Exact Stochastic Simulation of Chemical Systems with Many Species and Many Channels, *J. Phys. Chem. A*, **104** 9 1876–1889 (2000)
- ⁴⁵ S. Eugene, W-F. Xue, P. Robert and M. Doumic-Jauffret, Insights into the variability of nucleated amyloid polymerization by a minimalistic model of stochastic protein assembly, *hal-01205549*, (2015)
- ⁴⁶ F. Rezakhanlou, Gelation for MarcusLushnikov process, *Ann. Probab.*, **41** 3B (2013)
- ⁴⁷ N. Fournier and P. Laurençot, Marcus-Lushnikov processes, Smoluchowskis and Florys models, *Stoch. Proc. Appl.*, **119** 1 (2009)
- ⁴⁸ M. R. DOrsogna, Q. Lei and T. Chou, First assembly times and equilibration in stochastic coagulation-fragmentation, *J. Chem. Phys.*, **143** 1 (2015)
- ⁴⁹ The fact that the first aggregation rate need to be rescaled differently from the other aggregation rate comes from the special role played by the monomer in the BD and LS model. For a detailed discussion on the modelling point of view, see^{40,41}

Comment citer ce document :

Yvinec, R., Bernard, S., Hingant, E., Pujot-Menjouet, L. (2016). First passage times in homogeneous nucleation. Dependence on the total number of particles. The volume 473 of the series *Publications of the Institut Henri Poincaré*, PACS number(s) (02.50.Ga) B2160106387.49400337.10.Rt).